

Conversion of 3Fe-4S to 4Fe-4S Clusters in Native Pyruvate Formate-Lyase Activating Enzyme: Mössbauer Characterization and Implications for Mechanism

Carsten Krebs,[†] Timothy F. Henshaw,[§] Jennifer Cheek,[§] Boi Hanh Huynh,^{*,†} and Joan B. Broderick^{*,§}

Contribution from the Department of Chemistry, Michigan State University, East Lansing, Michigan 48824, and Department of Physics, Emory University, Atlanta, Georgia 30322

Received September 11, 2000

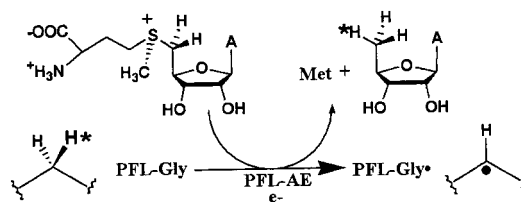
Abstract: Pyruvate formate-lyase activating enzyme utilizes an iron–sulfur cluster and *S*-adenosylmethionine to generate the catalytically essential glycy radical on pyruvate formate-lyase. Variable-temperature (4.2–200 K) and variable-field (0.05–8 T) Mössbauer spectroscopy has been used to characterize the iron–sulfur clusters present in anaerobically isolated pyruvate formate-lyase activating enzyme and in the dithionite-reduced form of the enzyme. Detailed analysis of the Mössbauer data indicates that the anaerobically isolated enzyme contains a mixture of Fe–S clusters with the cuboidal [3Fe-4S]⁺ clusters as the primary cluster form, accounting for 66% of the total iron. Other forms present include [2Fe-2S]²⁺ (12% of total Fe) and [4Fe-4S]²⁺ (8% of total iron). Careful examination of Mössbauer spectra recorded at various applied fields reveal a fourth spectral component which is assigned to a linear [3Fe-4S]⁺ (~10% of total Fe). Reduction of the as-isolated enzyme by dithionite, interestingly, converts all cluster types into the [4Fe-4S] form with a mixture of 2+ (66% of total iron) and 1+ (12% of total iron) oxidation states. These results are discussed in light of the proposed role for the iron–sulfur cluster in radical generation.

Introduction

Pyruvate formate-lyase (PFL) catalyzes the conversion of pyruvate and coenzyme A (CoA) to formate and acetyl-CoA, a key step in anaerobic glycolysis in facultative bacteria, such as *Escherichia coli*.^{1–4} PFL is a 170 kDa homodimeric protein which belongs to a group of enzymes that utilize protein radicals for catalysis.⁵ The active form of PFL contains a stable glycy radical located at residue 734.⁶ This catalytically essential protein radical is generated posttranslationally by a specific activating enzyme, pyruvate formate-lyase activating enzyme (PFL-AE), under anaerobic conditions in a reaction that is strictly dependent on the presence of *S*-adenosylmethionine (AdoMet) as a cosubstrate.^{7–9} During the PFL activation reaction, the glycy radical is formed by abstraction of the pro-S hydrogen atom of

G734 of PFL, and AdoMet is converted stoichiometrically to methionine and 5'-deoxyadenosine (5'-dAdo) (Scheme 1).^{10,11} Isotope-labeling experiments have established that the hydrogen atom abstracted from G734 is incorporated into the methyl group of the 5'-dAdo product, suggesting that a 5'-dAdo radical is the species that abstracts a hydrogen from G734.¹¹

Scheme 1



PFL-AE was initially purified to homogeneity by Conradt et al. and found to be a monomeric protein of about 30 kDa.¹ The catalytic activity of purified PFL-AE was shown to be strictly dependent on the addition of Fe(II) to the assay, and subsequently PFL-AE was described as an Fe-containing protein.² The purified enzyme exhibited a broad absorbance in the visible region (a peak at 388 nm and a shoulder at 430 nm) that was attributed to an unidentified organic cofactor.¹ Until recently, the nature of this unidentified chromophore has remained elusive, partly due to its sensitivity toward oxygen and partly due to the low abundance of PFL-AE in *E. coli*, both of which hindered detailed spectroscopic characterization.

* To whom correspondence should be addressed. J.B.B.: tel (517) 355-9715 ext 180; fax (517) 353-1793; E-mail broderij@cem.msu.edu. B.H.H.: tel (404) 727-4295; fax (404) 727-0873; E-mail vhuynh@emory.edu.

[†] Emory University.

[§] Michigan State University.

(1) Conradt, H.; Hohmann-Berger, M.; Hohmann, H. P.; Blaschkowski, H. P.; Knappe, J. *Arch. Biochem. Biophys.* **1984**, *228*, 133–142.

(2) Knappe, J.; Sawers, G. *FEMS Microbiol. Rev.* **1990**, *75*, 383–398.

(3) Knappe, J.; Elbert, S.; Frey, M.; Wagner, A. F. V. *Biochem. Soc. Trans.* **1993**, *21*, 731–734.

(4) Wong, K. K.; Kozarich, J. W. *Met. Ions Biol. Syst.* **1994**, *30*, 279–313.

(5) Stubbe, J.; van der Donk, W. A. *Chem. Rev. (Washington, D.C.)* **1998**, *98*, 705–762.

(6) Wagner, A. F. V.; Frey, M.; Neugebauer, F. A.; Schaefer, W.; Knappe, J. *Proc. Natl. Acad. Sci. U.S.A.* **1992**, *89*, 996–1000.

(7) Knappe, J.; Schacht, J.; Moeckel, W.; Hoepner, T.; Vetter, H., Jr.; Edenharder, R. *Eur. J. Biochem.* **1969**, *11*, 316–327.

(8) Knappe, J.; Blaschkowski, H. P.; Groebner, P.; Schmitt, T. *Eur. J. Biochem.* **1974**, *50*, 253–263.

(9) Knappe, J.; Schmitt, T. *Biochem. Biophys. Res. Commun.* **1976**, *71*, 1110–1117.

(10) Knappe, J.; Neugebauer, F. A.; Blaschkowski, H. P.; Gaenzler, M. *Proc. Natl. Acad. Sci. U.S.A.* **1984**, *81*, 1332–1335.

(11) Frey, M.; Rothe, M.; Wagner, A. F. V.; Knappe, J. *J. Biol. Chem.* **1994**, *269*, 12432–12437.

The limitation on the quantity of protein for comprehensive physical characterization was overcome when Wong et al. succeeded in cloning and overexpressing PFL-AE in *E. coli*.¹² The recombinant enzyme was purified from inclusion bodies under denaturing conditions followed by anaerobic refolding and was found to be active in the presence of added iron, although the specific activity (1.9 U/mg) was lower than that reported for wild-type PFL-AE (25 U/mg). (The unit definition proposed by Külzer et al.¹³ is used here.) The refolded protein did not exhibit absorption in the 400 nm region, suggesting a fundamental difference between this denatured/refolded protein and the wild-type enzyme purified by Conradt et al.¹ The recombinant apo PFL-AE could bind approximately one Fe(II) per protein monomer, and the Fe(II)-PFL-AE exhibited a visible absorption at 320 nm. Similar binding stoichiometry was found for other divalent metals, such as Cu(II) and Co(II), but only the Fe(II)-incorporated protein was capable of activating PFL.¹² Inhibition studies showed that thiophilic metals such as Cu(II), Zn(II), Hg(II), and Cd(II) were inhibitors of PFL activation,¹² consistent with an earlier suggestion that a cluster of three cysteines, C29, C33, and C36, might be ligands to the iron site.¹⁴

Recently, we identified PFL-AE as an iron-sulfur protein after purification of recombinant PFL-AE from the soluble fractions under anaerobic and nondenaturing conditions.¹⁵ The specific activity of this enzyme, though low (5.4 U/mg), was shown to correlate with the cluster content of the protein, indicating an essential role for the cluster in catalytic activity. The purified PFL-AE was characterized by using a range of spectroscopic methods, including optical, resonance Raman, MCD, and EPR spectroscopy.¹⁵ The results showed a mixture of [2Fe-2S]²⁺ and [4Fe-4S]²⁺ clusters in the as-isolated enzyme. Under dithionite-reducing conditions and in the absence of AdoMet, only [4Fe-4S]²⁺ clusters were detected by Raman spectroscopy. When PFL-AE was reduced in the presence of AdoMet, a nearly axial $S = 1/2$ EPR signal ($g = 2.013, 1.889,$ and 1.878) typical of [4Fe-4S]⁺ clusters was observed. These observations, together with the iron/sulfide/protein ratio, were interpreted at the time as suggesting the presence of a subunit-bridging [4Fe-4S]^{2+/+} cluster in the dithionite-reduced enzyme, with the [2Fe-2S]²⁺ clusters being a result of oxidative degradation of the cluster due to incomplete anaerobicity during purification.¹⁵ Based on more recent work from our laboratory and Knappe's laboratory, however, it seems unlikely that PFL-AE contains subunit-bridging [4Fe-4S] clusters (vide infra).

Külzer et al. have shown that apo PFL-AE can be reconstituted with Fe(II) and sulfide under reducing conditions, and the reconstituted PFL-AE exhibits a specific activity of 46 U/mg in the absence of added iron.¹³ This reconstituted enzyme is monomeric and contains primarily [4Fe-4S]²⁺ clusters as deduced from optical spectroscopy. These clusters can be partially reduced by dithionite both in the presence and in the absence of AdoMet, producing EPR signals characteristic of [4Fe-4S]⁺ clusters. The presence of AdoMet changes the EPR signal from an axial $S = 1/2$ signal ($g = 2.029$ and 1.925) to a rhombic signal ($g = 2.009, 1.921,$ and 1.886). Both [4Fe-4S]⁺ signals observed in the reconstituted enzyme are different from

what is observed for the anaerobically purified enzyme reduced by dithionite in the presence of AdoMet,¹⁵ suggesting subtle differences between reconstituted and native enzyme.

[Note: Throughout this paper, we use the term "native" to refer to PFL-AE that has been purified with an intact iron-sulfur cluster. In contrast, "reconstituted" enzyme has been treated with iron and sulfide prior to spectroscopic characterization.]

Although the above-mentioned investigations have established that PFL-AE is an iron-sulfur protein and have provided illuminative information concerning the properties of the Fe-S cluster that it contains, the methods used in these studies do not offer a complete description of the states of the cluster present in the enzyme. For example, resonance Raman spectroscopy is insensitive to the reduced [2Fe-2S]⁺ cluster, and EPR spectroscopy cannot detect diamagnetic clusters such as [2Fe-2S]²⁺ and [4Fe-4S]²⁺. In addition, quantitative information is difficult if not impossible to extract from resonance Raman data. Given the complex picture that is emerging for the Fe-S clusters in PFL-AE and other AdoMet-dependent iron-sulfur enzymes,¹⁶⁻¹⁸ a thorough and quantitative characterization of all cluster species present under different conditions is critical to further structural and mechanistic studies. Consequently, Mössbauer spectroscopy, a method that can detect and quantify each Fe species in the sample, is used here for a complete characterization of the iron-sulfur clusters in PFL-AE.

We have recently improved our expression system by subcloning the PFL-AE gene into an isopropyl- β -D-thiogalactopyranoside (IPTG)-inducible vector and thereby avoiding the possibly detrimental heat-induction step used in our earlier expression procedure.¹⁹ Since the Fe-S cluster in PFL-AE appears to be air sensitive, we have purified the enzyme under strictly anaerobic conditions by carrying out the purification steps in an anaerobic chamber (earlier work¹⁵ was done benchtop under a blanket of inert gas). Initial optical, Raman, and EPR characterizations indicate the presence of predominantly [3Fe-4S]⁺ cluster in the as-isolated enzyme with a stoichiometry of 2.5-3.0 Fe and S per monomer and a specific activity of 31 U/mg in the absence of added iron.¹⁹ We report here a detailed Mössbauer characterization of the as-isolated and dithionite-reduced forms of the purified enzyme. Consistent with the previous finding,¹⁹ the as-isolated enzyme contains primarily cuboidal [3Fe-4S]⁺ clusters. Minor portions of the Fe are present as mixtures of [2Fe-2S]²⁺, [4Fe-4S]²⁺, and linear [3Fe-4S]⁺ clusters. Reduction of the enzyme with dithionite converts most of the clusters into [4Fe-4S] clusters, of which the majority are in the diamagnetic 2+ state with a small amount in the 1+ state. No other Fe cluster species are detected. This report, together with our earlier communications,^{15,19} provides the only characterization of the iron-sulfur clusters present in PFL-AE in its native state without artificial reconstitution. Such studies are fundamental for obtaining a working understanding of the structural and functional properties of the Fe-S cluster in PFL-AE and are particularly significant given the recently determined role of the cluster in the generation of the G734 radical in PFL.²⁰

(16) Ollagnier, S.; Meier, C.; Mulliez, E.; Gaillard, J.; Schünemann, V.; Trautwein, A.; Mattioli, T.; Lutz, M.; Fontecave, M. *J. Am. Chem. Soc.* **1999**, *121*, 6344-6350.

(17) Tamarit, J.; Mulliez, E.; Meier, C.; Trautwein, A.; Fontecave, M. *J. Biol. Chem.* **1999**, *274*, 31291-31296.

(18) Ollagnier-de Choudens, S.; Sanakis, Y.; Hewitson, K. S.; Roach, P.; Baldwin, J. E.; Münck, E.; Fontecave, M. *Biochemistry* **2000**, *39*, 4165-4173.

(19) Broderick, J. B.; Henshaw, T. F.; Cheek, J.; Wojtuszewski, K.; Smith, S. R.; Trojan, M. R.; McGhan, R. M.; Kopf, A.; Kibbey, M.; Broderick, W. E. *Biochem. Biophys. Res. Commun.* **2000**, *269*, 451-456.

(20) Henshaw, T. F.; Cheek, J.; Broderick, J. B. *J. Am. Chem. Soc.* **2000**, *122*, 8331-8332.

(12) Wong, K. K.; Murray, B. W.; Lewis, S. A.; Baxter, M. K.; Ridky, T. W.; Ulissi-DeMario, L.; Kozarich, J. W. *Biochemistry* **1993**, *32*, 14102-14110.

(13) Külzer, R.; Pils, T.; Kappl, R.; Hüttermann, J.; Knappe, J. *J. Biol. Chem.* **1998**, *273*, 4897-4903.

(14) Rödel, W.; Plaga, W.; Frank, R.; Knappe, J. *Eur. J. Biochem.* **1988**, *177*, 153-158.

(15) Broderick, J. B.; Duderstadt, R. E.; Fernandez, D. C.; Wojtuszewski, K.; Henshaw, T. F.; Johnson, M. K. *J. Am. Chem. Soc.* **1997**, *119*, 7396-7397.

Materials and Methods

Bacterial Growth in ^{57}Fe -Enriched Medium and Protein Purification. PFL-AE used for Mössbauer studies was overexpressed and purified from BL21(DE3)pLysS/pCal-n-AE3 as previously described,¹⁹ except that both overnight and large-scale cultures were grown in a defined MOPS medium. The defined medium was based on one previously described²¹ but modified to include 0.5 mM CaCl_2 , 1% (w/v) casamino acids, and 0.001% (w/v) each of pyridoxine, riboflavin, niacinamide, folic acid, cyanocobalamin, pantothenic acid, and thioctic acid. The medium also contained 20 μM ^{57}Fe added from a concentrated solution obtained by dissolving the metal (94.7% enrichment) in a minimal volume of 2:3:1 $\text{H}_2\text{O}:\text{HCl}$ (concentrated): HNO_3 (concentrated). Protein, iron, and sulfide assays were done as previously described.^{19,22,23} Activity assays were performed in the absence of added iron as previously described,¹⁹ except that the production of the product PFL glycy radical was monitored directly by EPR spectroscopy. PFL-AE Mössbauer samples (0.51 mM for as-isolated, 0.49 mM final concentration for reduced) were prepared in an anaerobic chamber (MBraun) maintained at <1 ppm O_2 . The reduced samples were prepared at ambient temperature by addition of sodium dithionite to a final concentration of 1.28 mM. Addition of higher concentrations of dithionite (up to 5 mM) did not affect the amount of $[\text{4Fe-4S}]^+$ cluster obtained. No additional iron was added during reduction, so the $[\text{3Fe-4S}]$ -to- $[\text{4Fe-4S}]$ cluster conversions reported herein must occur by cannibalization of the destroyed clusters. Immediately after reduction, the samples were frozen by immersion in liquid nitrogen.

Mössbauer and EPR Spectroscopy. Mössbauer spectra were recorded in either a weak-field spectrometer equipped with a Janis 8DT variable-temperature cryostat or a strong-field spectrometer furnished with a Janis CNDT/SC SuperVaritemp cryostat encasing an 8-T superconducting magnet. Both spectrometers operate in a constant acceleration mode in a transmission geometry. The zero velocity of the spectra refers to the centroid of a room-temperature spectrum of a metallic iron foil. EPR spectra were recorded in a Bruker ER-200D-SRC spectrometer equipped with an Oxford Instruments ESR 910 continuous-flow cryostat.

Results

Fe Content. Preparations of the ^{57}Fe -enriched PFL-AE were analyzed for iron and protein content. The results show an iron to protein monomer ratio of 1.3 ± 0.1 . This value is lower than the 2.8 Fe/protein monomer reported for the enzyme purified from bacteria grown in terrific broth with naturally available Fe. Since the ^{57}Fe -enriched PFL-AE was isolated from bacteria grown in defined medium, this observed difference in Fe content may suggest inefficient incorporation of the Fe cluster under suboptimal growth conditions. Two observations, however, indicate that the only difference between ^{57}Fe -enriched and unenriched PFL-AE is the absolute quantity of iron incorporated, not the form in which it is incorporated. First, the EPR and UV-visible spectroscopic properties of ^{57}Fe -enriched PFL-AE are essentially identical to those of PFL-AE isolated from bacteria grown with naturally available Fe. Second, the specific activity of the ^{57}Fe -enriched PFL-AE containing 1.3 Fe per protein monomer (48 U/mg) is approximately half that for unenriched PFL-AE containing 2.65 Fe per protein monomer (95 U/mg). The specific activities reported here are higher than any previously published for PFL-AE. We previously reported 31 U/mg for PFL-AE with 2.8 Fe per protein,¹⁹ and Knappe has reported 46 U/mg for PFL-AE with 2.6 Fe per protein.¹³ The higher specific activities reported here are presumably a result of directly monitoring the formation of product PFL glycy radical as a function of time, rather than using the coupled enzyme assay previously described.^{13,19}

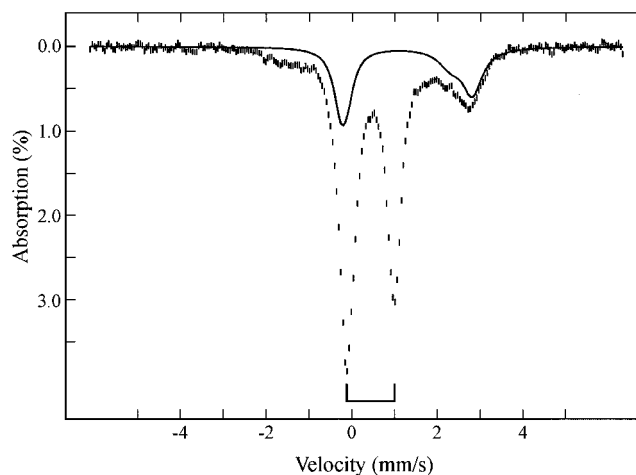


Figure 1. Mössbauer spectrum of dithionite-reduced native PFL-AE recorded at 4.2 K in a magnetic field of 0.05 T applied parallel to the γ -beam. The bracket indicates the positions of the quadrupole doublet arising from the $[\text{4Fe-4S}]^{2+}$ cluster. The solid line is the theoretical simulation of the adventitiously bound Fe(II) assuming two quadrupole doublets with $\delta(1) = 1.28$ mm/s, $\Delta E_Q(1) = 3.07$ mm/s, $\delta(2) = 1.10$ mm/s, and $\Delta E_Q = 2.42$ mm/s. Doublet 1 contributes 17% of the total Fe absorption, and doublet 2 contributes 8%.

Fe-S Cluster Composition in PFL-AE. Samples of the anaerobically purified ^{57}Fe -enriched PFL-AE in two different states (as-isolated and dithionite-reduced) were investigated by Mössbauer spectroscopy at various temperatures and applied fields. Both states contain mixtures of Fe species. The observed spectra are superpositions of the various spectra of the different species contained in the samples. We have therefore employed a self-consistent iterative approach to obtain a set of parameters for the different species such that all the spectra recorded under different conditions can be explained by the same set of parameters. In the following, we will present the results of the dithionite-reduced sample first because it contains fewer Fe species.

The 4.2 K Mössbauer spectrum of a dithionite-reduced PFL-AE sample (Figure 1), recorded in a magnetic field of 50 mT oriented parallel to the γ -beam, displays an intense central quadrupole doublet (marked by a bracket), a broad absorption peak at ~ 2.8 mm/s, and weak absorptions between -2 and $+2.5$ mm/s. These features are associated with three spectral components and thus represent three different Fe species. The broad absorption peak at ~ 2.8 mm/s is the high-energy line of a quadrupole doublet (shown as a solid line in Figure 1), of which the parameters (see legend of Figure 1) and shape are indicative of adventitiously bound high-spin Fe(II). Removal of the contribution of the adventitious Fe(II) (25% of the total Fe absorption) from the raw data reveals the spectrum arising from the Fe-S clusters (Figure 2A). The central quadrupole doublet, accounting for 66% of the total Fe absorption, is best simulated with two overlapping quadrupole doublets (dashed line in Figure 2A). The parameters used in the simulation are listed in Table 1 and are typical for $[\text{4Fe-4S}]^{2+}$ clusters.²⁴⁻²⁶ Without exception, $[\text{4Fe-4S}]^{2+}$ clusters have an $S = 0$ ground state, resulting from antiferromagnetic coupling of the two valence-delocalized Fe-(II)Fe(III) units. To examine the spin state of the species associated with the central doublet, a spectrum of the dithionite-

(24) Middleton, P.; Dickson, D. P. E.; Johnson, C. E.; Rush, J. D. *Eur. J. Biochem.* **1978**, *88*, 135-141.

(25) Middleton, P.; Dickson, D. P. E.; Johnson, C. E.; Rush, J. D. *Eur. J. Biochem.* **1980**, *104*, 289-296.

(26) Trautwein, A. X.; Bill, E.; Bominaar, E. L.; Winkler, H. *Struct. Bonding (Berlin)* **1991**, *78*, 1-95.

(21) Garboczi, D. N.; Hüllihen, J. H.; Pedersen, P. L. *J. Biol. Chem.* **1988**, *263*, 15694-15698.

(22) Beinert, H. *Methods Enzymol.* **1978**, *54*, 435-445.

(23) Beinert, H. *Anal. Biochem.* **1983**, *131*, 373-378.

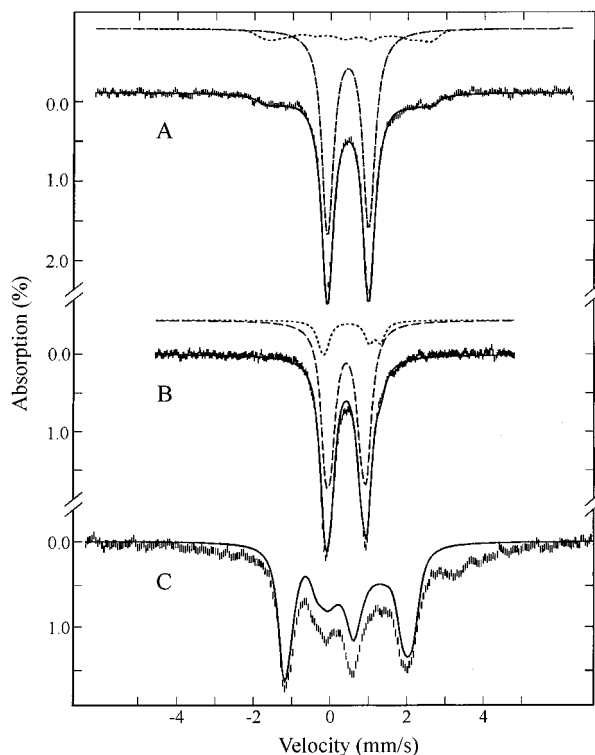


Figure 2. Mössbauer spectra of dithionite-reduced PFL-AE recorded at 4.2 K in a parallel field of 0.05 T (A), 170 K in the absence of applied field (B), and 4.2 K in a parallel field of 8 T (C). The contributions from the adventitiously bound Fe(II) have been removed for the spectra shown in A and B. The solid lines in A and B are summations of theoretical simulations of the $[4\text{Fe-4S}]^{2+}$ (dashed lines, 66% of total Fe absorption) and the $[4\text{Fe-4S}]^+$ (dotted lines, 12%) clusters. The solid line in C is the theoretical simulation of the $[4\text{Fe-4S}]^{2+}$ cluster, assuming diamagnetism.

Table 1. Temperature-Dependent Mössbauer Parameters of the Fe–S Clusters in Native PFL-AE^a

		T (K)		
		4.2	113	170
$[4\text{Fe-4S}]^{2+}$				
site 1	δ (mm/s)	0.45 (2)	0.44 (2)	0.42 (2)
	ΔE_Q (mm/s)	1.15 (4)	1.13 (4)	1.10 (4)
	η	0.3		
site 2	δ (mm/s)	0.45 (2)	0.44 (2)	0.42 (2)
	ΔE_Q (mm/s)	1.00 (4)	0.83 (4)	0.80 (4)
	η	0.7		
$[2\text{Fe-2S}]^{2+}$				
	δ (mm/s)	0.29 (2)	0.26 (2)	0.23 (2)
	ΔE_Q (mm/s)	0.58 (4)	0.58 (4)	0.58 (4)
	η	0		

^a Values in parentheses are uncertainties in units of the least significant digit.

reduced PFL-AE was recorded in a strong external field of 8 T at 4.2 K (Figure 2C). The solid line plotted over the data in Figure 2C is a simulation using the parameters obtained for the central doublet from the weak-field spectrum and assuming diamagnetism. The agreement between the simulation and the central portion of the experimental spectrum confirms that the central doublet is arising from a diamagnetic species. Thus, this component is assigned to a $[4\text{Fe-4S}]^{2+}$ cluster.

The component having absorption extending from -2 to 2.5 mm/s, which accounts for 12% of the total Fe absorption, is originating from a paramagnetic species and can be attributed to a $[4\text{Fe-4S}]^+$ cluster with an $S = 1/2$ ground state. Mössbauer

spectra of such clusters consist of two equal intensity subspectra representing a valence-delocalized Fe(II)Fe(III) pair and a diferrous pair.^{24,26} Because of the weak intensity and because the number of variables required for spectral simulation of a $[4\text{Fe-4S}]^+$ cluster is large, we did not attempt to determine the specific parameters for the $[4\text{Fe-4S}]^+$ cluster in the dithionite-reduced PFL-AE by fitting this paramagnetic component. Instead, to show that this paramagnetic component is consistent with that of a $[4\text{Fe-4S}]^+$ cluster, we have used the parameters obtained for the $[4\text{Fe-4S}]^+$ cluster of *Bacillus stearothermophilus* ferredoxin²⁴ to simulate a spectrum for comparison with this component. The simulation is plotted in Figure 2A as a dotted line. It can be seen that the magnetic splitting and shape of the paramagnetic component in PFL-AE agree well with the simulation. Addition of the simulated $[4\text{Fe-4S}]^+$ spectrum (12%) with the least-squares fit spectrum for the $[4\text{Fe-4S}]^{2+}$ cluster (66%) generates the solid line overlaid with the experimental spectrum shown in Figure 2A. The agreement observed between the theory and the experimental spectrum supports the above assignment.

At high temperatures the electronic relaxation of a $[4\text{Fe-4S}]^+$ cluster is fast in comparison with the Larmor frequency of the ^{57}Fe nucleus, resulting in cancellation of the internal field and collapse of the low-temperature magnetic spectrum into two quadrupole doublets associated with the Fe(II)Fe(III) and the diferrous pairs.^{24,26} Figure 2B shows a spectrum of the dithionite-reduced PFL-AE recorded at 170 K in the absence of an applied field (the contribution of the adventitiously bound Fe(II) has been removed from the spectrum shown). As expected, the paramagnetic component observed at 4.2 K has collapsed into quadrupole doublets at this temperature. A small shoulder at ~ 1.3 mm/s is observed. A comparison with the simulated spectrum of the *B. stearothermophilus* $[4\text{Fe-4S}]^+$ cluster²⁴ at this temperature (dotted line in Figure 2B) indicates that this shoulder is at the position of the high-energy line of the quadrupole doublet of the diferrous pair. The intensity of this shoulder is also consistent with the percent absorption (12% of total Fe absorption) determined for the $[4\text{Fe-4S}]^+$ cluster from the low-temperature data. To demonstrate that the high-temperature spectrum is in agreement with the assignment made from analyzing the low-temperature data, we have again added the simulated central doublet (long-dashed line in Figure 2B for the $[4\text{Fe-4S}]^{2+}$ cluster) and the simulated *B. stearothermophilus* $[4\text{Fe-4S}]^+$ spectrum (dotted line) according to the intensities determined from the low-temperature spectra (66% for the $[4\text{Fe-4S}]^{2+}$ and 12% for the $[4\text{Fe-4S}]^+$) and plotted the sum (solid line) over the experimental spectrum. The agreement between the simulation and experiment indicates that both the high-temperature and low-temperature Mössbauer data are consistent with the conclusion that, except for the adventitiously bound Fe(II), only $[4\text{Fe-4S}]$ clusters are present in the dithionite-reduced PFL-AE. The percent absorption of the $[4\text{Fe-4S}]$ cluster determined from the Mössbauer measurement, together with the iron and protein determinations, yields a stoichiometry of ~ 0.25 $[4\text{Fe-4S}]$ cluster per protein monomer, of which 85% are in the diamagnetic $[4\text{Fe-4S}]^{2+}$ state and the remainder are in the paramagnetic $[4\text{Fe-4S}]^+$ state.

The presence of a small quantity of $[4\text{Fe-4S}]^+$ cluster in the dithionite-reduced PFL-AE is also supported by EPR measurements. An X-band EPR spectrum of a dithionite-reduced PFL-AE prepared in parallel with the Mössbauer sample displays an axial $S = 1/2$ signal with g values at 2.01 and 1.94 (Figure 3). This signal is very similar to that reported for the dithionite-reduced reconstituted PFL-AE.¹³ Double integration of this

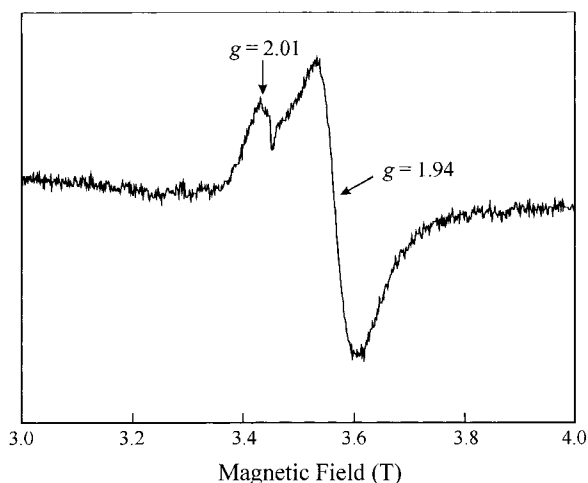


Figure 3. EPR spectrum of dithionite-reduced PFL-AE showing a weak signal originating from the $[4\text{Fe-4S}]^+$ cluster. The spectrum was recorded with the following instrumental settings: temperature, 12 K; microwave power, 2 mW; microwave frequency, 9.65 GHz; modulation amplitude, 1 mT; modulation frequency, 100 kHz.

signal yields a spin quantitation of 0.03–0.04 spin/protein monomer, a value that is consistent with the Mössbauer finding of ~ 0.04 $[4\text{Fe-4S}]^+$ cluster per protein monomer.

Figure 4A shows a Mössbauer spectrum of the as-isolated PFL-AE recorded at 4.2 K in a parallel applied field of 50 mT. At least three spectral components are discernible from this spectrum. The major component, which accounts for 66% of the Fe absorption, displays magnetic hyperfine interactions with absorption extending from -2 to 3 mm/s (solid line plotted above the data). This component is composed of three equal-intensity subspectral components and exhibits field-orientation and field-strength dependence consistent with an $S = 1/2$ electronic system (vide infra). At temperatures above 77 K, this magnetic component collapses into a quadrupole doublet (Figure 4B) with parameters ($\delta = 0.23$ mm/s and $\Delta E_Q = 0.58$ mm/s at 170 K) typical of tetrahedral sulfur-coordinated high-spin Fe(III). All these features are characteristic of the all-ferric cuboidal $[3\text{Fe-4S}]^+$ cluster. This magnetic component is thus assigned to such a cluster. This assignment is consistent with our previous EPR finding that the majority of the Fe–S cluster in the as-isolated PFL-AE is in an $S = 1/2$ $[3\text{Fe-4S}]^+$ state.¹⁹ Detailed analysis of this magnetic component is presented in the following section.

A second spectral component accounting for 12% of the total Fe absorption is a sharp quadrupole doublet observed at 4.2 K (dashed line plotted above the data in Figure 4A) with parameters (listed in Table 1) characteristic of $[2\text{Fe-2S}]^{2+}$ clusters.^{26,27} Spectra recorded at strong applied field indicate that this component originates from a diamagnetic species. On the basis of this observed diamagnetism and the characteristic parameters, this component is assigned to a $[2\text{Fe-2S}]^{2+}$ cluster. Removal of the contributions of the $[3\text{Fe-4S}]^+$ and $[2\text{Fe-2S}]^{2+}$ clusters from the raw data reveals a third component identical to that of the $[4\text{Fe-4S}]^{2+}$ cluster observed in the dithionite-reduced PFL-AE (dotted line plotted above the data in Figure 4A). The high-energy line of this doublet can be seen as a shoulder at ~ 1 mm/s in the raw data. This component is estimated to account for $\sim 8\%$ of the total Fe absorption. A sum of the three components (the $[3\text{Fe-4S}]^+$, $[2\text{Fe-2S}]^{2+}$, and $[4\text{Fe-4S}]^{2+}$) yields the solid line plotted over the data in Figure 4A.

Although the agreement between the experiment and the simulated sum spectrum is reasonable, approximately 14% of the Fe absorption remains not accounted for. Spectra recorded at strong applied field reveal the presence of a fourth component (vide infra).

The complexity of the above-discussed low-temperature spectrum is greatly reduced when data are collected at high temperatures. This is due to the fact that, at high temperature, the $[3\text{Fe-4S}]^+$ cluster exhibits a single quadrupole doublet,²⁸ and this doublet is similar to that of a $[2\text{Fe-2S}]^{2+}$ cluster since both clusters are composed of only Fe(III) S_4 units. As expected, the 170 K spectrum of the as-isolated PFL-AE (Figure 4B) shows predominantly a quadrupole doublet arising from both the $[3\text{Fe-4S}]^+$ and $[2\text{Fe-2S}]^{2+}$ clusters (dashed line in Figure 4B). This central doublet accounts for 80% of the total Fe absorption, consistent with the sum of the amounts of these two types of clusters determined at 4.2 K. The presence of a small quantity of the $[4\text{Fe-4S}]^{2+}$ cluster is supported by the appearance of a shoulder at the high-energy line of the central doublet. To illustrate this point, we plot in Figure 4B a simulated spectrum (dotted line in Figure 4B) of the $[4\text{Fe-4S}]^{2+}$ cluster using the parameters determined from the dithionite-reduced sample (Table 1). The plotted spectrum is normalized to 8% of the total Fe absorption. Addition of the simulated central quadrupole doublet with the simulated $[4\text{Fe-4S}]^{2+}$ doublet yields the solid line overlaid with the experimental data. Again, reasonable agreement between experiment and simulation is observed.

The fourth spectral component is readily observed in a spectrum recorded at 4.2 K in a parallel field of 4 T (Figure 4D). This component is seen as a magnetic spectrum with its outermost lines appearing at approximately -5 and 5 mm/s (indicated by arrows). In a much weaker (0.05 T) or stronger (8 T) applied field (Figure 4, spectra C and E, respectively), however, this magnetic component becomes broad and is difficult to detect. This field-strength dependence and the observed magnetic splitting are consistent with those of a linear $[3\text{Fe-4S}]^+$ cluster.^{29,30} In the following, we use the results obtained for the linear $[3\text{Fe-4S}]^+$ cluster in aconitase²⁹ as an example to illustrate this point and to compare with the PFL-AE spectra. For a linear $[3\text{Fe-4S}]^+$ cluster, the three $S = 5/2$ Fe(III) sites are spin-coupled to form an $S = 5/2$ ground state. The spin of the middle Fe site (site 3) is antiparallel to those of the two terminal Fe sites (sites 1 and 2). Consequently, the internal field of site 3 is parallel to the applied field, while those of the other two sites oppose the applied field. For the linear $[3\text{Fe-4S}]^+$ cluster in aconitase,²⁹ the observed internal fields for sites 1, 2, and 3 are -33.6 , -31.9 , and 24.2 T, respectively. The signs indicate the direction of the internal field in relation to that of the applied field. At 0.05 T, since all three internal fields are different in magnitude, the spectra arising from the three Fe sites show different magnetic splittings. Superposition of these three spectra results in a relatively broad spectrum (solid line overlaid with the experimental spectrum in Figure 4C). At 4 T, to a good approximation, the magnitudes of the effective fields at sites 1 and 2 are reduced by 4 T to 29.6 and 27.9 T, respectively, while that of site 3 is increased to 28.2 T. These values are quite similar, and thus, all three sites show similar magnetic spectra, superposition of which results in a “single” magnetic spectrum with its intensity tripled (solid line in Figure

(28) Huynh, B. H.; Kent, T. A. *Adv. Inorg. Biochem.* **1984**, *6*, 163–223.

(29) Kennedy, M. C.; Kent, T. A.; Emptage, M.; Merkle, H.; Beinert, H.; Münch, E. *J. Biol. Chem.* **1984**, *259*, 14463–71.

(30) Girerd, J. J.; Papaefthymiou, G. C.; Watson, A. D.; Gamp, E.; Hagen, K. S.; Edelstein, N.; Frankel, R. B.; Holm, R. H. *J. Am. Chem. Soc.* **1984**, *106*, 5941–5947.

(27) Ferreira, G. C.; Franco, R.; Lloyd, S. G.; Pereira, A. S.; Moura, I.; Moura, J. J. G.; Huynh, B. H. *J. Biol. Chem.* **1994**, *269*, 7062–7065.

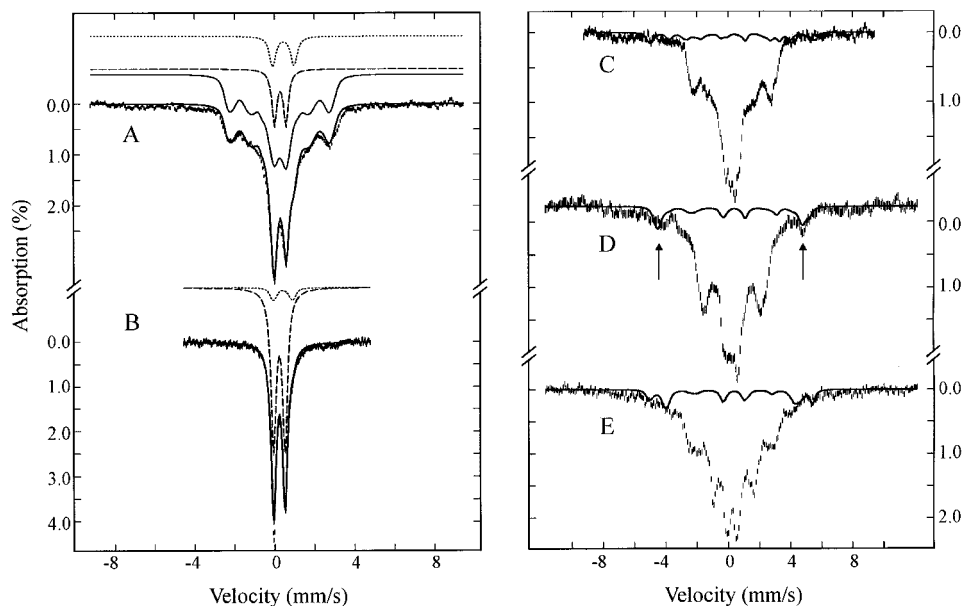


Figure 4. Mössbauer spectra of anaerobically purified native PFL-AE. The spectra were recorded at 4.2 K in a parallel field of 0.05 T (A and C), 170 K in zero field (B), 4.2 K in a parallel field of 4 T (D), or 8 T (E). For the spectra shown in C, D, and E, contributions from the [4Fe-4S]²⁺ (8%) and [2Fe-2S]²⁺ (12%) clusters have been removed. The solid line overlaid with the experimental spectrum in A is the sum of the theoretical simulations of the cuboidal [3Fe-4S]⁺ (solid line above the experimental spectrum, 66%), [2Fe-2S]²⁺ (dashed line, 12%), and [4Fe-4S]²⁺ (dotted line, 8%) clusters. The solid line in B is the sum of the quadrupole doublets arising from the [4Fe-4S]²⁺ cluster (dotted line above the experimental spectrum) and from the cuboidal [3Fe-4S]⁺ and [2Fe-2S]²⁺ (dashed line) clusters. The solid lines shown in C, D, and E are theoretical simulations of the linear [3Fe-4S]⁺ cluster using the parameters given in ref 29. The arrows in D indicate the positions at which the outermost lines of the three Fe sites of the linear [3Fe-4S]⁺ cluster overlap at 4 T (see text).

4D). At 8 T, the magnitudes of the effective fields at sites 1, 2, and 3 are again different, and a broad magnetic spectrum is again observed (solid line in Figure 4E). On the basis of the above analysis, it is concluded that the as-isolated PFL-AE contains linear [3Fe-4S]⁺ clusters, accounting for approximately 10% of the total iron absorption.

In summary, analysis of the Mössbauer data of the as-isolated PFL-AE shows the presence of mixtures of Fe-S clusters. A majority of the clusters are present in the cuboidal [3Fe-4S]⁺ state (~0.29 cluster/protein monomer), while minor portions are in the [2Fe-2S]²⁺ (~0.08 cluster/monomer), [4Fe-4S]²⁺ (~0.03 cluster/monomer), and linear [3Fe-4S]⁺ (~0.04 cluster/monomer) states.

Analysis of the [3Fe-4S]⁺ Spectral Component. Figure 5 shows the field-dependent spectra of the [3Fe-4S]⁺ cluster in the as-isolated PFL-AE. The spectra shown were prepared from the raw data by removing proper amounts of the contributions of the [2Fe-2S]²⁺ (12%), [4Fe-4S]²⁺ (8%), and linear [3Fe-4S]⁺ clusters (10%). To analyze these field-dependent spectra, we use a spin-coupling model commonly applied to [3Fe-4S]⁺ clusters.³¹ In this model, the three Fe sites are assumed to be intrinsically equivalent: a tetrahedral sulfur-coordinated $S = 5/2$ Fe(III). These three $5/2$ spins, S_1 , S_2 , and S_3 , are exchange-coupled according to eq 1, resulting in an $S = 1/2$ ground state that displays three equal-intensity subspectral components with different magnetic hyperfine interactions. Within this coupling

$$H_{\text{ex}} = J_{12} \mathbf{S}_1 \cdot \mathbf{S}_2 + J_{23} \mathbf{S}_2 \cdot \mathbf{S}_3 + J_{13} \mathbf{S}_1 \cdot \mathbf{S}_3 \quad (1)$$

scheme, there are only two orthogonal $S = 1/2$ states, which may be constructed by coupling spins S_2 and S_3 to form an intermediate spin $S_{23} = 2$ or 3, and then coupling S_{23} to S_1 to form the system spin $S = 1/2$. These two states may be

represented by the ket vectors $|S_{23}, S_1, S\rangle = |2, 5/2, 1/2\rangle$ and $|3, 5/2, 1/2\rangle$. For $J_{23} > J_{12} = J_{13} > 0$, the ground state is the pure $|2, 5/2, 1/2\rangle$ state. In the more general situation in which all three J values are different ($J_{23} > J_{12} > J_{13}$), the ground state is a quantum admixture of these two states, $(1 - \alpha^2)^{1/2} |2, 5/2, 1/2\rangle + \alpha |3, 5/2, 1/2\rangle$, and the spin expectation values for the three iron sites are functions of the mixing coefficient α^2 (eq 2 and Figure 6).

$$\begin{aligned} \langle S_{1z} \rangle &= \frac{7}{6} - 2\alpha^2 \\ \langle S_{2z} \rangle &= \alpha^2 - \frac{1}{3} - \sqrt{3}\alpha\sqrt{1 - \alpha^2} \\ \langle S_{3z} \rangle &= \alpha^2 - \frac{1}{3} + \sqrt{3}\alpha\sqrt{1 - \alpha^2} \end{aligned} \quad (2)$$

The observed magnetic hyperfine constants, A_i ($i = 1, 2$, and 3), for the three spin-coupled iron sites are given by

$$A_i = 2\langle S_{iz} \rangle a_i \quad (3)$$

where a_i is the magnetic hyperfine constant for the i th iron site in the absence of spin-spin coupling. Previous Mössbauer investigations of several [3Fe-4S]⁺ cluster-containing proteins have assumed substantially anisotropic hyperfine interaction for the iron sites in order to explain the relatively broad low-temperature Mössbauer spectra.^{32–37} Anisotropic hyperfine

(32) Emptage, M. H.; Kent, T. A.; Huynh, B. H.; Rawlings, J.; Orme-Johnson, W. H.; Münck, E. *J. Biol. Chem.* **1980**, *255*, 1793–1796.

(33) Huynh, B. H.; Moura, J. J. G.; Moura, I.; Kent, T. A.; LeGall, J.; Xavier, A. V.; Münck, E. *J. Biol. Chem.* **1980**, *255*, 3242–3244.

(34) Kent, T. A.; Dreyer, J. L.; Kennedy, M. C.; Huynh, B. H.; Emptage, M. H.; Beinert, H.; Münck, E. *Proc. Natl. Acad. Sci. U.S.A.* **1982**, *79*, 1096–1100.

(35) Surerus, K. K.; Kennedy, M. C.; Beinert, H.; Münck, E. *Proc. Natl. Acad. Sci. U.S.A.* **1989**, *86*, 9846–9850.

(31) Kent, T. A.; Huynh, B. H.; Münck, E. *Proc. Natl. Acad. Sci. U.S.A.* **1980**, *77*, 6574–6576.

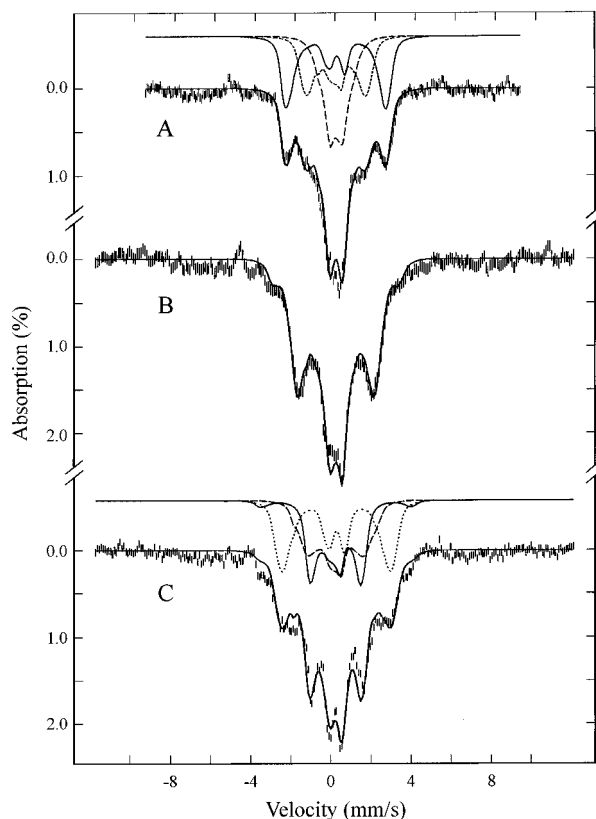


Figure 5. Mössbauer spectra of the cuboidal $[3\text{Fe-4S}]^+$ cluster in anaerobically purified PFL-AE. The spectra are recorded at 4.2 K with a parallel field of 0.05 T (A), 4 T (B), or 8 T (C). These spectra were prepared by removing from the raw data the contributions from the $[2\text{Fe-2S}]^{2+}$, $[4\text{Fe-4S}]^{2+}$, and linear $[3\text{Fe-4S}]^+$ clusters. The solid lines overlaid with the experimental spectra are theoretical simulations using the parameters given in text. In A and C, theoretical simulations for the individual Fe sites are also shown above the experimental data: site 1, solid lines; site 2, dotted lines; site 3, dashed lines.

interaction, however, is unusual for high-spin ferric ions. In particular, for monomeric high-spin ferric ions with tetrahedral sulfur coordination, the magnetic hyperfine interaction is rather isotropic (within 5%).^{38,39} In our analysis of the $[3\text{Fe-4S}]^+$ cluster in PFL-AE, we have chosen a more reasonable assumption and assumed isotropic a values for all three Fe sites. To reproduce the broad low-temperature spectra, we assumed the presence of Gaussian distributions in the exchange coupling constants J_{ij} . Since mixing of the two $S = 1/2$ states depends on the exchange couplings, distributions in the J_{ij} values would result in a distribution in the mixing coefficient α^2 , $P(\alpha^2)$, which in turn generates distributions in the magnetic hyperfine interactions (see eqs 2 and 3) and causes broadening of the spectrum. Detailed analysis of the data shows that this approach not only can explain the low-temperature weak-field spectrum (Figure 5A) but also can reproduce the field-dependent behavior of the spectra up to 8 T (assuming anisotropic magnetic hyperfine interaction cannot reproduce the field-dependent behavior of the $[3\text{Fe-4S}]^+$ spectra in the range 0.05–8 T).

(36) Teixeira, M.; Moura, I.; Xavier, A. V.; Moura, J. J. G.; LeGall, J.; DerVartanian, D. V.; Peck, H. D., Jr.; Huynh, B. H. *J. Biol. Chem.* **1989**, *264*, 16435–16450.

(37) Surerus, K. K.; Chen, M.; van der Zwaan, J. W.; Rusnak, F. M.; Kolk, M.; Duin, E. C.; Albracht, S. P. J.; Münck, E. *Biochemistry* **1994**, *33*, 4980–4993.

(38) Schulz, C.; Debrunner, P. G. *J. Phys. (Paris), Colloq.* **1976**, 153–158.

(39) Moura, I.; Huynh, B. H.; Hausinger, R. P.; Le Gall, J.; Xavier, A. V.; Münck, E. *J. Biol. Chem.* **1980**, *255*, 2493–8.

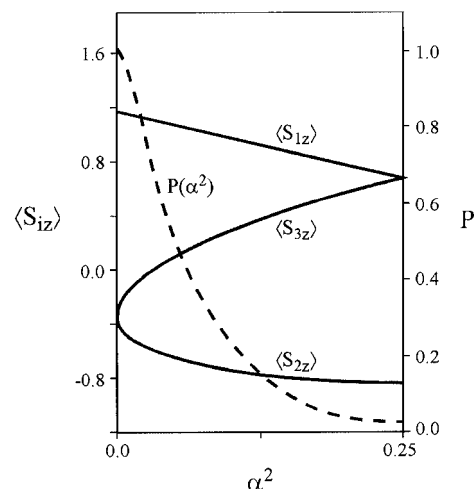


Figure 6. Spin expectation values for the three Fe sites of a $[3\text{Fe-4S}]^+$ cluster plotted as functions (solid lines) of the mixing coefficient α^2 according to eq 2, and the distribution of α^2 , $P(\alpha^2)$ (dashed line), calculated with the assumed J_{ij} distributions described in text.

Theoretical simulations resulting from this analysis are plotted in Figure 5 as solid lines overlaid with the experimental spectra. Simulations of the individual spectral components (for the three iron sites) are also shown above the 0.05-T (A) and 8-T (C) spectrum. The parameters used in these simulations are $\delta = 0.28$ mm/s, $\Delta E_Q = 0.60$ mm/s, $\eta = 0$, and line width = 0.35 mm/s for all three sites, $a_1/g_n\beta_n = -13.8$ T, $a_2/g_n\beta_n = a_3/g_n\beta_n = -13.1$ T, $J_{12} = 296$ cm^{-1} , $J_{13} = 300$ cm^{-1} , $J_{23} = 323$ cm^{-1} , and $\sigma_{12} = \sigma_{13} = \sigma_{23} = 5.3$ cm^{-1} , where σ_{ij} is the Gaussian standard deviation for the corresponding J_{ij} . The intrinsic a values determined for the three Fe sites are consistent with those expected for Fe–S clusters.⁴⁰ The distribution in α^2 , $P(\alpha^2)$, calculated from the assumed distributions in J_{ij} , is plotted in Figure 6 as a dashed line. On the basis of saturation magnetization⁴¹ and temperature-dependent NMR⁴² studies of the $[3\text{Fe-4S}]^+$ -containing *Desulfovibrio gigas* ferredoxin II, we have chosen the J_{ij} values at around 300 cm^{-1} . The exact values used, however, are not important for our analysis because the mixing parameter α is dependent on the ratios of the three J_{ij} 's and not on their individual values. What is significant is that extremely narrow distributions ($\sigma_{ij}/J_{ij} \approx 1.2\%$) for the exchange coupling constants are sufficient to generate the observed broad distributions in magnetic hyperfine interactions. We have learned recently that distributions in the J_{ij} values have also been used successfully to describe the field-dependent Mössbauer spectra of *D. gigas* Fd II (Eckard Münck, personal communication).

Discussion

PFL-AE has previously been shown to require the presence of an iron–sulfur cluster to catalyze the generation of the glycol radical of PFL and the concomitant cleavage of AdoMet to methionine and 5'-deoxyadenosine.^{13,15,19,20} The exact nature of the cluster has remained elusive, however, as $[2\text{Fe-2S}]$, $[3\text{Fe-4S}]$, and $[4\text{Fe-4S}]$ clusters have been detected in different forms of the enzyme and under different conditions. Herein we report for the first time a comprehensive examination of the cluster

(40) Mouesca, J.-M.; Noodleman, L.; Case, D. A.; Lamotte, B. *Inorg. Chem.* **1995**, *34*, 4347–4359.

(41) Day, E. P.; Peterson, J.; Bonvoisin, J. J.; Moura, I.; Moura, J. J. G. *J. Biol. Chem.* **1988**, *263*, 3684–3689.

(42) Macedo, A. L.; Moura, I.; Moura, J. J. G.; Le Gall, J.; Huynh, B. H. *Inorg. Chem.* **1993**, *32*, 1101–1105.

forms present in reduced and oxidized PFL-AE using Mössbauer spectroscopy, the only technique capable of identifying and quantifying all cluster forms simultaneously. The work described here provides important new insights into the nature of the iron–sulfur cluster in PFL-AE and its possible role in radical generation.

In PFL-AE under reducing conditions, all iron–sulfur clusters are present in the [4Fe-4S] form. With dithionite as reductant as described here, a majority of these clusters are in the diamagnetic [4Fe-4S]²⁺ state, with a small amount present as [4Fe-4S]⁺ clusters. Both oxidation states of the cluster are identified by Mössbauer spectroscopy, with the quantitation of the paramagnetic [4Fe-4S]⁺ confirmed by parallel EPR studies. These results corroborate previous work suggesting that the primary cluster form after dithionite reduction is [4Fe-4S]²⁺.¹⁵ In recent work, we have shown that deazariboflavin-mediated photoreduction of PFL-AE followed by addition of AdoMet produces primarily [4Fe-4S]⁺.²⁰ Regardless of the reducing conditions, however, only cuboidal [4Fe-4S] clusters are observed upon reduction of the enzyme. This observation suggests that the [4Fe-4S] is the catalytically relevant cluster, since PFL-AE catalytic activity is observed in vitro only under anaerobic reducing conditions.¹ In support of this, we have recently provided direct evidence for the catalytic relevance of the [4Fe-4S]^{2+/+} states of PFL-AE.²⁰

In the as-isolated form of PFL-AE, essentially every form of cluster previously identified in this enzyme is present simultaneously, including cuboidal [3Fe-4S]⁺ as the dominant cluster form, as well as [2Fe-2S]²⁺ and [4Fe-4S]²⁺ clusters. In addition to these three cluster types, Mössbauer spectroscopy also provides evidence for the presence of a small amount of linear [3Fe-4S]⁺ cluster. The linear [3Fe-4S]⁺ structure type was first identified in synthetic iron–sulfur complexes^{30,43} and was later found to be present in a partially unfolded form of aconitase.²⁹ This structure type remains quite rare in biological systems, however, and to our knowledge has not been identified in any proteins other than aconitase. The identification of linear [3Fe-4S]⁺ clusters in PFL-AE, together with the observation of the other three cluster forms (cuboidal [3Fe-4S]⁺, [2Fe-2S]²⁺, and [4Fe-4S]²⁺), makes PFL-AE remarkably similar to aconitase in its ability to accommodate all these cluster types.²⁹

The linear [3Fe-4S]⁺ and [2Fe-2S]²⁺ clusters were generated as the predominant cluster forms of aconitase by incubation of the protein at high pH or in high concentrations of urea, conditions under which the protein is believed to be partially unfolded.²⁹ Our observation of a small amount of linear [3Fe-4S]⁺ and [2Fe-2S]²⁺ clusters in PFL-AE therefore suggests that a small amount of our as-isolated native PFL-AE may be partially unfolded. As with aconitase, however, reduction of PFL-AE with dithionite converts these [3Fe-4S] and [2Fe-2S] clusters to [4Fe-4S] clusters. Some of us have also shown that, under alternate conditions of growth, expression, and purification of PFL-AE, the [2Fe-2S]²⁺ can be a major cluster form, but upon reduction this form converts to solely [4Fe-4S] clusters.¹⁵ By analogy to aconitase, the [2Fe-2S] cluster observed as a major component of our previous preparations may have been due to partial unfolding of PFL-AE. For PFL-AE, a significant amount of the [2Fe-2S] cluster was observed under conditions in which (1) overexpression was achieved by heat-induction, which could result in partial protein unfolding, and (2) the protein was not kept strictly anaerobic during purification (crudely anaerobic conditions were maintained by purging

buffers with argon), which could have allowed oxidative degradation of the cluster and partial protein unfolding.¹⁵ Our current use of a non-heat-inducible expression system, coupled with purification in an anaerobic chamber, has apparently allowed isolation of PFL-AE containing a more native-like structure, as judged by the predominance of the cuboidal [3Fe-4S]⁺ cluster form. An important conclusion of these results is that, regardless of whether the predominant form in the as-isolated PFL-AE is [2Fe-2S]²⁺ or [3Fe-4S]⁺, reduction under anaerobic conditions results in conversion to the active [4Fe-4S] cluster form.

The most significant similarity between PFL-AE and aconitase lies in the implication of a unique iron site of the [4Fe-4S] cluster. The ready accessibility of a [3Fe-4S]⁺ cluster from a native [4Fe-4S] cluster, as has been found for both PFL-AE and aconitase,³⁴ as well as *Pyrococcus furiosus* ferredoxin⁴⁴ and *Desulfovibrio africanus* ferredoxin III,⁴⁵ is indicative of a site-differentiated [4Fe-4S] cluster.⁴⁶ A site-differentiated [4Fe-4S] cluster has been demonstrated in aconitase, where addition of Fe(II) to the [3Fe-4S]⁺ form of the enzyme results in incorporation of the added iron into a single site of the cluster.^{47–49} Oxidation of the resulting [4Fe-4S] cluster results in loss of iron exclusively from the unique site. The labile iron site of aconitase was thus labeled with ⁵⁷Fe and shown to have Mössbauer parameters distinct from those of the three other sites in the cluster.⁴⁷ Furthermore, Mössbauer and ENDOR spectroscopy reveal that substrate coordinates to this unique site in the aconitase ES complex, thus indicating a specific functional role for the labile iron site.^{47,50,51} An analogous unique iron site in the [4Fe-4S] of PFL-AE is suggested by the observation that the major cluster form of as-isolated PFL-AE is [3Fe-4S]⁺, and that reduction of this cluster converts it quantitatively to the active [4Fe-4S] cluster form. Further Mössbauer studies are underway to characterize the unique site of the PFL-AE [4Fe-4S] cluster.

In support of the above suggested site-differentiated [4Fe-4S] cluster in PFL-AE, site-directed mutagenesis studies have shown that PFL-AE, like aconitase,^{52,53} has only three cysteines implicated in cluster coordination.¹³ In the absence of substrate or product, the fourth ligand to the [4Fe-4S] cluster in aconitase is solvent.⁴⁷ The fourth ligand to the [4Fe-4S] cluster in PFL-AE has yet to be identified, but by analogy to aconitase it is reasonable to propose that exogenous ligands such as water or substrate may bind to the unique labile iron site in PFL-AE. Evidence suggests that the other Fe–S/AdoMet enzymes may also contain a [4Fe-4S] cluster with one unique iron site. A putative cluster-binding motif comprised of only *three* cysteines (CX₃CX₂C) is common to all of the Fe–S/AdoMet-dependent enzymes for which the gene sequence is known,^{14,54–58} implying that a fourth ligand to the [4Fe-4S] cluster in these enzymes

(44) Conover, R. C.; Kowal, A. T.; Fu, W.; Park, J. B.; Aono, S.; Adams, M. W. W.; Johnson, M. K. *J. Biol. Chem.* **1990**, *265*, 8533–8541.

(45) George, S. J.; Armstrong, F. A.; Hatchikian, E. C.; Thomson, A. J. *Biochem. J.* **1989**, *264*, 275–284.

(46) Johnson, M. K.; Duderstadt, R. E.; Duin, E. C. *Adv. Inorg. Chem.* **1999**, *47*, 1–82.

(47) Emptage, M. H.; Kent, T. A.; Kennedy, M. C.; Beinert, H.; Münck, E. *Proc. Natl. Acad. Sci. U.S.A.* **1983**, *80*, 4674–4678.

(48) Kennedy, M. C.; Emptage, M. H.; Dreyer, J. L.; Beinert, H. *J. Biol. Chem.* **1983**, *258*, 11098–11105.

(49) Emptage, M. H.; Dreyer, J. L.; Kennedy, M. C.; Beinert, H. *J. Biol. Chem.* **1983**, *258*, 11106–11111.

(50) Werst, M. M.; Kennedy, M. C.; Beinert, H.; Hoffman, B. M. *Biochemistry* **1990**, *29*, 10526–10532.

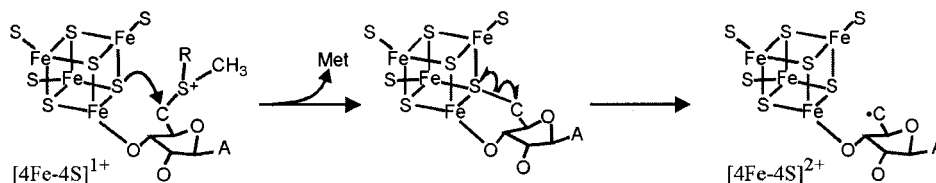
(51) Werst, M. M.; Kennedy, M. C.; Houseman, A. L. P.; Beinert, H.; Hoffman, B. M. *Biochemistry* **1990**, *29*, 10533–10540.

(52) Plank, D. W.; Howard, J. B. *J. Biol. Chem.* **1988**, *263*, 8184–8193.

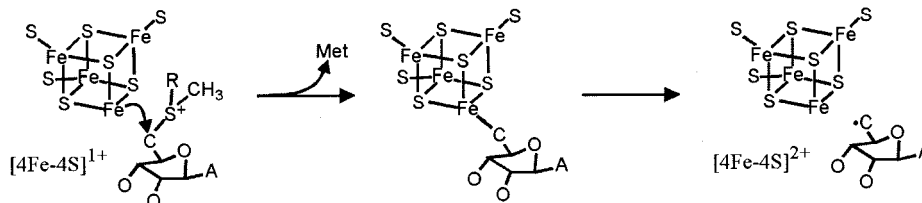
(53) Kennedy, M. C.; Beinert, H. *J. Biol. Chem.* **1988**, *263*, 8194–8198.

(43) Hagen, K. S.; Watson, A. D.; Holm, R. H. *J. Am. Chem. Soc.* **1983**, *105*, 3905–3913.

Scheme 2



Scheme 3



may not be a cysteine. In some cases, such as biotin synthase, spectroscopic evidence supports the presence of one non-cysteine ligand to the [4Fe-4S] cluster.⁵⁹ In other cases, such as lysine aminomutase,⁶⁰ anaerobic ribonucleotide reductase,^{61,62} and PFL-AE, evidence for [3Fe-4S]⁺ clusters has been obtained. The common three-cysteine-cluster binding motif, together with much of the available spectroscopic data, suggests that a structurally and functionally important aspect of the iron-sulfur cluster in these enzymes is the presence of a unique iron site in the [4Fe-4S] cluster.

The Fe-S/AdoMet enzymes appear to operate by a common mechanism involving reduction of the [4Fe-4S] cluster followed by reaction with AdoMet to yield methionine and a 5'-deoxyadenosyl radical, which then generates a substrate radical by hydrogen atom abstraction. The mechanism by which the Fe-S cluster and AdoMet interact to generate a 5'-deoxyadenosyl radical is currently not understood. The observation presented here suggested a unique iron site in PFL-AE and led us to propose possible mechanisms that involve the unique iron site for the generation and stabilization of the 5'-deoxyadenosyl radical. One possible role for the unique iron site could be coordination of AdoMet through the ribose O-3 atom (Scheme 2). Such coordination could position the 5'-C of AdoMet in a conformation favorable for nucleophilic attack by one of the μ -3 sulfides of the cluster, thereby facilitating leaving of methionine and generation of the putative intermediate adenosyl radical (Scheme 2). Coordination of a ribose hydroxyl of AdoMet to an iron of the cluster would be analogous to the ligation of substrate-derived O atom(s) to the unique iron site in aconitase.⁶³ The coordination of AdoMet to an iron of the cluster, as shown in Scheme 2, would also account for the significant

alteration of the EPR properties of the [4Fe-4S]⁺ cluster in the presence of AdoMet.¹³ In essence, the μ -3 sulfide mediates electron transfer to the substrate via formation of a covalent adduct. The covalent cluster-adenosyl complex (Scheme 2, center) can be thought of as a "protected" adenosyl radical, much like the latent adenosyl radical in adenosylcobalamin. The unusual sulfur-based cluster chemistry shown in Scheme 2 is similar to that proposed earlier for lysine aminomutase.⁶⁴ A similar mechanism has also been proposed for ferredoxin: thioredoxin reductase (FTR), in which nucleophilic attack by a μ -3 sulfide of a [4Fe-4S]⁺ cluster resulted in reductive cleavage of the disulfide bond.^{65,66} A recent X-ray structure of FTR, however, shows a close distance (3.1 Å) between a cluster iron and a sulfur atom of the active-site disulfide, suggesting an alternative mechanism for cleaving the disulfide bond through interaction with the cluster iron.⁶⁷

A variation of the mechanism shown in Scheme 2 would involve one of the coordinated cysteines, rather than a μ -3 sulfide, acting as the nucleophile. The nucleophilic character of coordinated cysteines has been demonstrated in small-molecule models of biological iron-sulfur clusters, where electrophiles have been shown to react with [4Fe-4S] clusters to give alkylated thiols derived from cluster ligands.^{68,69} The precedent for nucleophilic coordinated thiols lends credence to the possibility of nucleophilic chemistry for the cysteines of PFL-AE. However, the presence of only three cysteine ligands to the [4Fe-4S] cluster of PFL-AE requires that cluster intermediates with only two cysteine ligands are generated. To our knowledge, there are no examples of biological [4Fe-4S] clusters with only two cysteine ligands. Furthermore, coordination of the O-3 of AdoMet to the unique Fe site of the cluster, as proposed above, would not position the 5'-C of AdoMet for efficient nucleophilic attack by one of the coordinated cysteines. This mechanism would therefore leave no obvious role for the

(54) Sun, X.; Eliasson, R.; Pontis, E.; Andersson, J.; Buist, G.; Sjoeborg, B.-M.; Reichard, P. *J. Biol. Chem.* **1995**, *270*, 2443–2446.

(55) Otsuka, A. J.; Buoncristiani, M. R.; Howard, P. K.; Flamm, J.; Johnson, C.; Yamamoto, T.; Uchida, K.; Cook, C.; Ruppert, J.; Matsuzaki, J. *J. Biol. Chem.* **1988**, *263*, 19577–19585.

(56) Hayden, M. A.; Huang, I.; Bussiere, D. E.; Ashley, G. W. *J. Biol. Chem.* **1992**, *267*, 9512–9515.

(57) Fajardo-Cavazos, P.; Salazar, C.; Nicholson, W. L. *J. Bacteriol.* **1993**, *175*, 1735–1744.

(58) Ruzicka, F. J.; Lieder, K. W.; Frey, P. A. *J. Bacteriol.* **2000**, *184*, 469–476.

(59) Duin, E. C.; Lafferty, M. E.; Crouse, B. R.; Allen, R. M.; Sanyal, I.; Flint, D. H.; Johnson, M. K. *Biochemistry* **1997**, *36*, 11811–11820.

(60) Petrovich, R. M.; Ruzicka, F. J.; Reed, G. H.; Frey, P. A. *Biochemistry* **1992**, *31*, 10774–10781.

(61) Liu, A.; Gräslund, A. *J. Biol. Chem.* **2000**, *275*, 12367–12373.

(62) Mulliez, E.; Ollagnier-de Choudens, S.; Meier, C.; Cremonini, M.; Luchinat, C.; Trautwein, A. X.; Fontecave, M. *J. Biol. Inorg. Chem.* **1999**, *4*, 614–620.

(63) Beinert, H.; Kennedy, M. C.; Stout, C. D. *Chem. Rev.* **1996**, *96*, 2335–2373.

(64) Frey, P. A.; Reed, G. H. *Adv. Enzymol. Relat. Areas Mol. Biol.* **1993**, *66*, 1–39.

(65) Staples, C. R.; Ameyibor, E.; Fu, W.; Gardet-Salvi, L.; Stritt-Etter, A.-L.; Schuermann, P.; Knaff, D. B.; Johnson, M. K. *Biochemistry* **1996**, *35*, 11425–11434.

(66) Staples, C. R.; Gaynard, E.; Stritt-Etter, A.-L.; Telser, J.; Hoffman, B. M.; Schuermann, P.; Knaff, D. B.; Johnson, M. K. *Biochemistry* **1998**, *37*, 4612–4620.

(67) Dai, S.; Schwendtmayer, C.; Schuermann, P.; Ramaswamy, S.; Eklund, H. *Science (Washington, D.C.)* **2000**, *287*, 655–658.

(68) Johnson, R. W.; Holm, R. H. *J. Am. Chem. Soc.* **1978**, *100*, 5338–5344.

(69) Wilker, J. J.; Lippard, S. J. *Inorg. Chem.* **1999**, *38*, 3569–3574.

unique iron site that appears to be a common feature of the adenosylmethionine-dependent Fe/S enzymes.

Another possible role for the unique iron site in the [4Fe-4S] cluster of PFL-AE is based on similarities to the adenosylcobalamin (AdoCbl) enzymes.⁵ The Fe-S/AdoMet and AdoCbl-dependent enzymes are the only enzymes for which 5'-deoxyadenosyl radicals have been implicated as key reaction intermediates. For both groups of enzymes, the central mechanistic step involves abstraction of a hydrogen atom from substrate by the adenosyl radical intermediate. In the case of the AdoCbl-dependent enzymes, the adenosyl radical intermediate is generated by homolytic cleavage of the weak Co-C bond of AdoCbl. It is therefore intriguing to consider the possibility that the unique iron site of the cluster interacts directly with the 5'-C atom of AdoMet during the PFL-AE-catalyzed reaction, forming an analogous organometallic intermediate, involving a direct bond between the 5'-C of the adenosyl moiety and the unique iron site (Scheme 3). The adenosyl radical intermediate could then be generated by homolytic cleavage of the Fe-C bond.

The investigation of the adenosylmethionine-dependent iron-sulfur enzymes is a rapidly evolving area of study, as new members of this group of enzymes are uncovered and the functional and spectroscopic details of each of the enzymes are pursued. These enzymes have in common a CX₃CX₂C cluster

binding motif, but little other sequence homology. The nature of the iron-sulfur clusters in these enzymes has been an area of intense research and has revealed complex relationships between 2Fe, 3Fe, and 4Fe cluster forms that are affected by the isolation methods, reconstitution, and presence of oxidants or reductants. The present work has provided the first clear description of all of the cluster forms present in native PFL-AE and has provided important insight into possible catalytic mechanisms. The chemistry catalyzed by the adenosylmethionine-dependent iron-sulfur enzymes is amazingly diverse, including cofactor biosynthesis, DNA repair, rearrangement reactions, and generation of stable protein radicals; however, a common mechanistic step appears to be hydrogen atom abstraction mediated by a 5'-deoxyadenosyl radical intermediate. The work reported here suggests that a site-differentiated [4Fe-4S] cluster may be present in these enzymes and could play an important role in binding and activating adenosylmethionine for adenosyl radical generation.

Acknowledgment. This work was supported by grants from the NIH (GM54608 to J.B.B. and GM47295 to B.H.H.) and Research Corporation (CC4057 to J.B.B.) and by setup funds provided by Michigan State University (to J.B.B.).

JA003335P